

A SECOND INTERACTION REGION FOR GAMMA-GAMMA, GAMMA-ELECTRON AND ELECTRON-ELECTRON COLLISION[†]

Kwang-Je Kim
for the Second Interaction Region Collaboration*
Lawrence Berkeley National Laboratory, Berkeley, CA 94720

Abstract

A design of a possible second interaction region (IR2) for $\gamma\gamma$, γe^- and e^-e^- collisions for the next linear collider (NLC) is presented. In the IR2, high energy photon beams are produced via Compton backscattering of focused laser beams by the high energy electron beams and brought into collision with the opposing electron or photon beams. With the goal of obtaining the $\gamma\gamma$ luminosity of about $10^{33}\text{cm}^{-2}\text{s}^{-1}$ within a 20% bandwidth, we use the electron beams parameters for the NLC e^+e^- design, but modify, the final focus optics. An array of optical mirrors brings the laser beam into a tight focus 5 mm upstream of the interaction point. The laser required must have about a TW of peak power and tens of kW of average power and can be either a solid state laser or a free electron laser.

1 INTRODUCTION

Figure 1 shows the schematic illustration of the IR2. In the following, we describe a summary of a preliminary design of the IR2 for the NLC at 500 GeV energy. A detailed description is given in Appendix B to the Zeroth Order Design Report for the NLC[1]. The major parameters are summarized in Table 1. A review of $\gamma\gamma$ and γe^- colliders, machine designs and physics applications, can be found in the proceedings of a workshop at Berkeley[2].

2 THE SCHEME

The laser beam must be chosen to optimize the generation of the γ -rays via Compton scattering at the CP[3]. About $n_\gamma=65\%$ of the high energy electrons are "converted" to γ -photons with the laser parameters in Table 1. The non-linear effects which may spoil the conversion process by shifting the γ -photons to lower energy and producing pairs through non-linear Breit-Wheeler process, etc., are small but not negligible.

The total $\gamma\gamma$ luminosity is approximately given by $n_\gamma^2 \approx 0.4$ times the geometric e^-e^- luminosity. The spectral luminosity depends strongly on the distance b between the CP and the IP; when $b=0$, it is broadly

Table 1. Major parameters

<u>Electron beam parameters</u>	
Luminosity goal	$\sim 10^{33}\text{cm}^{-2}\text{s}^{-1}$ for 20% BW
	$\sim 5 \times 10^{33}\text{cm}^{-2}\text{s}^{-1}$ for broad band
Beam parameters before FFS	The same as e^+e^- design
Electron energy	250 GeV
Rep. rate	90 bunches separated by 1.4 ns, 180 Hz
Particles per bunch	$N_e=0.65 \times 10^{10}$
Normalized rms emittance	$\gamma\epsilon_x=5 \times 10^{-6}$ mr, $\gamma\epsilon_y=8 \times 10^{-8}$ mr
Beta function at the IP	$\beta_x^* = \beta_y^* = 0.5$ mm
Rms spotsize at the IP	$\sigma_x^* = \sigma_y^* = 71.5 / 9.04$ nm
Rms bunch length	$\sigma_z=0.1$ mm
Polarization	Fully polarized with helicity switching capability
CP-IP distance	$b = 5$ mm
<u>Laser parameters</u>	
Wavelength	$\lambda = 1.053$ μm
Micropulse energy	$A = 1$ J
Rms spotsize at waist	$\sigma_{Lx} = \sigma_{Ly} = 2.90$ μm
Rms angular divergence	$\sigma_{Lx} = \sigma_{Ly} = 28.9$ mr
Rms micropulse length	$\sigma_{Lz} = 0.23$ mm
Peak intensity	$\approx 1 \times 10^{18}\text{W}/\text{cm}^2$
Peak power	0.5 TW
Average power	16.2 kW
Transverse coherence	Near diffraction limited
Polarization	Fully polarized with helicity switching capability

distributed as a function of the c.m. energy of the two-photon system. As b is increased, the low-energy part of the luminosity spectrum becomes suppressed due to the larger spot size occupied by low-energy photons. For most applications, one would choose $b \approx \gamma\sigma_y^*$, where σ_y^* is the vertical rms spotsize, to obtain a well defined peak of luminosity spectrum at the high-energy end with a bandwidth of about 20% without suffering a large luminosity reduction. In our case, this correspond to $b \sim 5$ mm. The spectral peak at the high-energy end, which is also characterized by a high degree of polarization, acco-

[†] Work supported by the U.S. Department of Energy under Contract no. DE-AC03-76SF00098.

* K. van Bibber, S. Chattopadhyay, W. Fawley, D. Helm, T. Houck, J. Irwin, K.-J. Kim, D. Klem, D. Meyerhofer, H. Murayama, M. Perry, M. Ronan, A. Sessler, T. Takahashi, V. Telnov, A. Weidemann, G. Westenskow, M. Xie, K. Yokoya, A. Zholents.

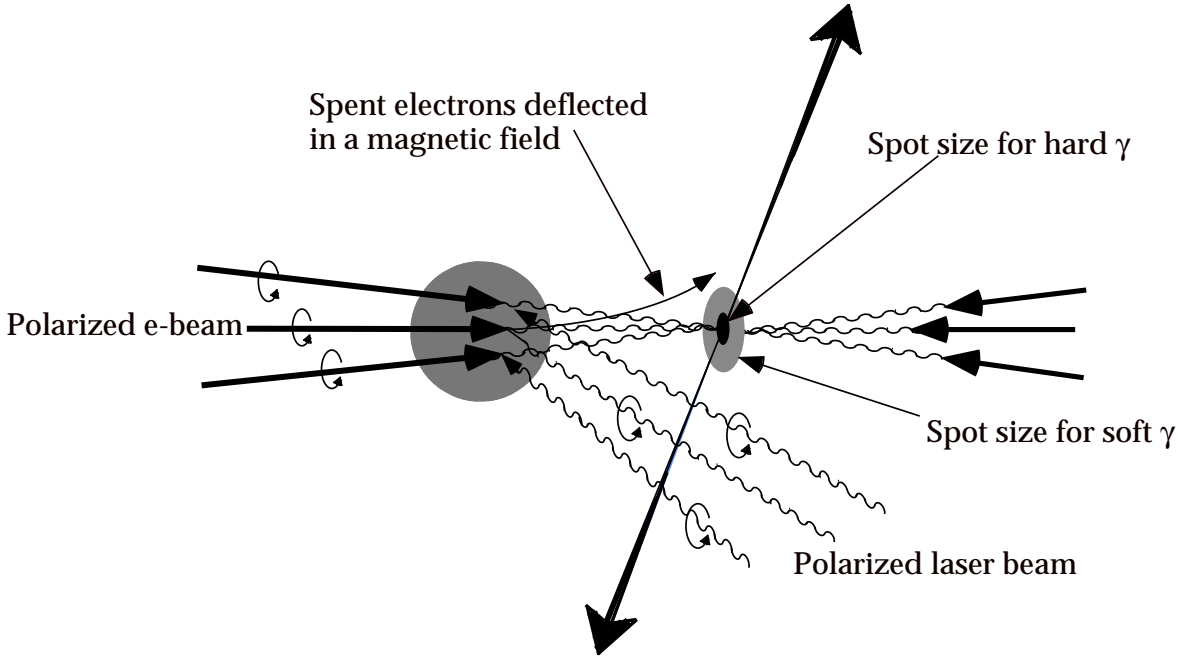


Figure 1: General scheme of gamma-gamma collision.

units for about 20% of the total $\gamma\gamma$ luminosity, or about 10% of the geometrical e-e- luminosity.

For e^+e^- collisions, the beam spot at the IP is normally designed to be flat to minimize the beamstrahlung effect. In $\gamma\gamma$ collision, the effective vertical beam size is larger than that in the e+e- collisions for a reasonable value of the CP-IP distance b . Thus the FFS for $\gamma\gamma$ collision must provide a value of β_x^* smaller and β_y^* larger than the corresponding values for the e^+e^- design. We aim for $\beta_x^*=\beta_y^*=0.5\text{mm}$ for the IR2.

The electron beams, if allowed to proceed to the IP, will contribute a large γe background events in $\gamma\gamma$ collisions. A way to avoid the collision of the spent electron beams would be to sweep them away from the IP by an external magnetic field. The magnetic field should extend longitudinally to about 1 cm with a strength of about 1 T. Such a magnet could be designed with a pulsed conductor[4].

3 LUMINOSITY CALCULATIONS

In our preliminary calculation, we have used Telnov's code extensively, which includes the multiple scattering effects in linear approximation and the same-profile approximation for Compton scattering at CP, deflection by external magnetic field and synchrotron radiation in the region between the CP and the IP, the beamstrahlung and the coherent pair production at the IP. A similar code has been assembled by Takahashi[5] based on Ohgaki's Compton conversion package and ABEL[6]. A more refined code incorporating Yokoya's non-linear Compton conversion and the ABEL-MOD[7] is being assembled as a collaborative effort between Hiroshima University, KEK, SLAC and LBNL. This code is referred to as CAIN

1.1. Recently, Yokoya has written a new code, named CAIN 2.0[6].

The results of luminosity calculations can be summarized as follows: We have considered the cases for the collisions at various vertical offset Δy without the sweeping magnet, and the case where there is a 1-T sweeping magnet. The distance between the CP and the IP is taken to be 7.8mm for the latter case. The $\gamma\gamma$ luminosity at high energy end, $z>0.65$, is about 10% of the geometric luminosity. Here z is the invariant mass of the colliding system/energy of the incoming electrons. A significant fraction of the total $\gamma\gamma$ luminosity is therefore in the low-energy region, and arises from the collisions of the beamstrahlung photons generated at the IP by the interaction of the spent electron beams. The luminosity distributions are not a very sensitive function of the offset Δy . The $\gamma\gamma$ luminosity at high energy end ($z>0.65$) is practically constant. Therefore the tolerance on Δy is rather relaxed; Δy up to about $1\sigma_y^*$ does not degrade the collision performance. The background from the low energy $\gamma\gamma$ or γe^- luminosities are significantly reduced when the sweeping magnet is employed.

4 LASER OPTICAL PATH

Figure 2 illustrates a possible mirror arrangement for the $\gamma\gamma$ collision region of the NLC. The figure shows the inner radius of the vertex chamber surrounding the IP, the conical mask, the quadrupole holders indicated by two cylinders, the incoming electron beam path indicated by a line nearly parallel to the axis, and the outgoing, disrupted electron beam path indicated by a narrow cone emanating from the IP next to the incoming beam path. The small elliptical objects are the mirrors. One of the laser beams

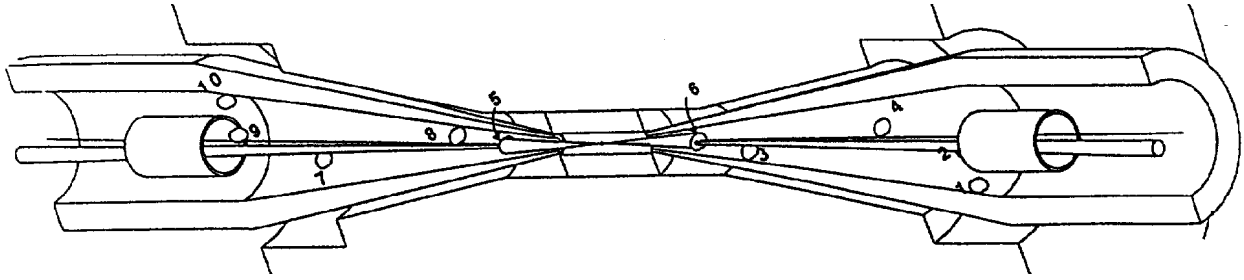


Figure 2: A possible mirror arrangement for the gamma-gamma collision.

enters from the right, and reflected by mirrors in sequence indicated by the numbers. The laser beam avoids the mirror 6 standing between the mirrors 4 and 5 by forming a focus a small distance away from the edge of mirror 6. The beam fills mirror 5 with a near uniform intensity profile, and focus on the CP with a $f/7$ optics facing the incoming electron beam from the right. Mirror 5 has two holes, a small one for the incoming electron beam and a larger one to accommodate the 10 mr angular cone of the outgoing disrupted electron beam. The laser beam further propagates and fills mirror 6, reflected and focused now to a spot a small distance away from the bottom edge of mirror 5 propagates further to mirrors 7, 8, 9, and 10, and exits to the left. Another laser beam enters from the left following a path symmetric to the beam coming from the right, nearly overlapping the exiting beam.

The mirrors will be of dielectric material with suitable multilayer coatings developed for high power laser systems. A laser path arrangement in which a laser pulse is reused several times will greatly reduce the optical power requirement. Practical implementation of these ideas need to be worked out.

5 ELECTRON FINAL FOCUS SYSTEM

The goal of the FFS for the IR2 is to produce $\beta_x^* = \beta_y^* = 0.5\text{mm}$, as explained in Section 2. As a first attempt to design the final focus system for $\gamma\gamma$ collisions, kept chromaticity of the final focus doublet close to the chromaticity of the e^+e^- final focus. Thus, with $L^* = 2\text{m}$, the minimum beam-stay-clear requirement of $10\sigma_{x,y}$, and the maximum pole-tip field in the permanent magnet quadrupoles of 1.35 T, we arrived at reasonable doublet parameters, the quadrupole nearest to the IP being of the F-type. However, the current version of the $\gamma\gamma$ final focus system has $\beta_x^* = 0.9\text{mm}$ and $\beta_y^* = 0.7\text{mm}$. The increase of the beam spot size at the IP due to the Oide effect is negligible. Following a standard approach to the chromaticity compensation the length FFS is 1600m. Efforts to find smaller b^* values resulted in higher x and y chromaticities, implying a greater sensitivity to the quadrupole placement tolerance and also a greater complexity and length of the FFS. By increasing the overall length of the Final Focus section to 1750m, we

found a solution giving $\beta_x^* = \beta_y^* = 0.5\text{mm}$ with the energy bandwidth about $\pm 0.5\%$.

6 LASER TECHNOLOGY

While the energy, pulse duration, and focusing can be met with currently operating lasers, based on the chirped pulse amplification technique[9,10], these lasers have not yet met the average power requirements. The average power of high peak power systems has, however, been increasing rapidly recently, driven by activities such as the Isotope Separation program at LLNL and facilitated by the development of high power laser diode pump sources. It is expected that the system requirements will be met with a series of 1-kW, diode-pumped, solid-state, chirped pulse amplification laser systems. These unit cells will be fed by a single, phase-locked oscillator to insure timing stability.

There are several options for the 1 kW unit cell: 1) direct, diode-pumped Nd:Glass based lasers incorporating advanced athermal glass, 2) direct, diode-pumped, broad-bandwidth crystals specially engineered for high average power applications (e.g., Yb:S-FAP or others) and, 3) two-stage laser-pumped lasers such as a long pulse (≈ 10 ns) neodymium based laser pumping a short-pulse Ti:Sapphire laser.

Free-electron lasers (FEL) are another option for photon colliders, and they are especially interesting for higher energy colliders, where the required wavelength of the laser is longer than $\sim 1 \mu\text{m}$, for which solid-state lasers do not presently exist. A scheme based on the chirped pulse amplification in a high-gain FEL driven by an induction linac appears promising[11].

REFERENCES

- [1] ZDR Report for NLC, SLAC, May 1996.
- [2] Nucl. Instr. Meth. A 355, 1-194 (1995).
- [3] V. Telnov, Nucl. Instr. Meth. A 355, 3 (1995)
- [4] G. Silvestrov and V. Telnov, unpublished.
- [5] T. Takahashi, in preparation.
- [6] K. Yokoya, KEK-Report 85-9, October 1985.
- [7] T. Tauchi, K. Yokoya, P. Chen, Par. Acc.41,29(1993).
- [8] User's Manual of CAIN 2.0 (KEK pub. 4/96).
- [9] D. Strickland, G. Mourou, Opt. Com.56, 219(1985).
- [10] M. Perry and G. Mourou, Science 264, 917 (1994).
- [11] K.-J. Kim, M. Xie and A. Sessler, LBL-37094.